J. Fluid Mech. (2002), *vol.* 470, *pp.* 223–245.
DOI: 10.1017/S0022112002001945 Printed in the United Kingdom

Wind forcing in the equilibrium range of wind-wave spectra

By TETSU HARA† AND STEPHEN E. BELCHER

Department of Meteorology, University of Reading, Reading RG6 6BB, UK

(Received 8 February 2000 and in revised form 10 January 2002)

A new analytical model is developed for the equilibrium range of the spectrum of wind-forced ocean surface gravity waves. We first show that the existing model of Phillips (1985) does not satisfy overall momentum conservation at high winds. This constraint is satisfied by applying recent understanding of the wind forcing of waves. Waves exert a drag on the air flow so that they support a fraction of the applied wind stress, which thus leaves a smaller turbulent stress near the surface to force growth of shorter wavelength waves. Formulation of the momentum budget accounting for this sheltering constrains the overall conservation of momentum and leads to a local turbulent stress that reduces as the wavenumber increases. This local turbulent stress then forces wind-induced wave growth. Following Phillips (1985), the wind sea is taken to be a superposition of linear waves, and equilibrium is maintained by a balance between the three sources and sinks of wave action.

These assumptions lead to analytical formulae for the local turbulent stress and the degree of saturation, $B(k)$, of waves in the equilibrium range. We identify a sheltering wavenumber, k_s, over which the local turbulent stress is significantly reduced by longer waves. At low wavenumbers or at low winds, when $k \ll k_s$, the sheltering is weak and $B(k)$ has a similar form to the model of Phillips (1985). At higher wavenumbers or at higher winds, $k \gg k_s$, $B(k)$ makes a transition to being proportional to k^0. The additional constraint of conservation of momentum also yields a formula for the coefficient that appears in the solution for $B(k)$. The spectra for mature seas are calculated from the model and are shown to agree with field observations. In particular, our model predicts more realistic spectral levels toward the high wavenumber limit compared to the previous model of Phillips (1985).

We suggest that the model may explain the overshoot phenomena observed in the spectral energy levels as the fetch increases.

1. Introduction

It is well known that, under given wind forcing, the spectra of ocean surface gravity waves attain an equilibrium state at frequencies much higher than the peak frequency (e.g. Phillips 1977, p. 140). Knowledge of the equilibrium range of the wave spectrum is of practical importance since existing numerical wave prediction models cannot solve right down to the smallest gravity waves. Instead, they resolve explicitly only to a fixed maximum wavenumber and then patch on to the spectrum a 'tail' to represent the equilibrium range (e.g. Komen *et al.* 1994, p. 234). Therefore, these models need to know the solution for the equilibrium range before being integrated.

† Permanent address: Graduate School of Oceanography, University of Rhode Island, Narragansett, RI 02882, USA.

We begin with a brief review of the observational evidence for an equilibrium range and of the salient aspects of recent models. This review suggests shortcomings, which are addressed in this paper.

1.1. *Observations of equilibrium spectra*

Early observational studies reported that the frequency wave height spectrum $\Phi(\sigma)$ in the equilibrium range was inversely proportional to the fifth power of the frequency σ

$$\Phi(\sigma) \propto g^2\sigma^{-5}, \tag{1.1}$$

where g is the acceleration due to gravity. Later, the JONSWAP report (Hasselmann *et al.* 1973) indicated that the coefficient of proportionality in (1.1) was a function of fetch rather than an absolute constant. Toba (1973), on the other hand, proposed that the wave height spectrum was better represented in the form of

$$\Phi(\sigma) \propto u_* g\sigma^{-4}, \tag{1.2}$$

where u_* is the wind friction velocity. This form received further support by other field observations. Donelan, Hamilton & Hui (1985) proposed a form of the frequency spectrum that was also proportional to σ^{-4}, but depended on the wave age rather than the friction velocity. In the mean time, Forristall (1981) reported that in the spectral range up to the frequency $\sigma \sim 0.17g/u_*$ the frequency spectrum was consistently proportional to σ^{-4}, while at higher frequencies the inverse fifth power law ($\propto \sigma^{-5}$) seemed to hold.

In the wavenumber domain, the wave height spectrum is defined in terms of the two-dimensional wavenumber vector $\boldsymbol{k}$ and is expressed as $\Psi(\boldsymbol{k})$ or $\Psi(k,\theta)$, where k is the magnitude of $\boldsymbol{k}$ and θ is the wave propagation direction. The only observational study in the wavenumber domain was reported by Banner, Jones & Trinder (1989) who found the one-dimensional wavenumber wave height spectrum $\Psi(k)$ in the form of

$$\Psi(k) = \int_{-\pi/2}^{\pi/2} \Psi(k,\theta)\,\mathrm{d}\theta \propto k^{-4}, \tag{1.3}$$

with the constant of proportionality almost independent of the wind stress. This form implies a frequency spectrum that is proportional to σ^{-5} if the linear dispersion relation is assumed.

In summary, there remain discrepancies in the form of the equilibrium spectra among different observations. Furthermore, it has become increasingly evident that the actual relationship between a frequency spectrum and a wavenumber spectrum is more subtle than that determined by the linear dispersion relation. Possible reasons are that the frequency spectrum can be modified by Doppler shifting of the shorter waves by advection by the orbital motion of dominant waves (Kitaigorodskii, Krasitskii & Zaslavskii 1975; Banner 1990), and because the frequency spectrum of bound higher harmonics of steep dominant waves may exceed the spectrum of freely propagating shorter waves (Belcher & Vassilicos 1997).

1.2. *Theories of equilibrium spectra*

Many models have been proposed to explain the nature and form of the equilibrium range; but there remain significant gaps in our current knowledge. The evolution of surface waves is described in terms of the spectral density of wave action, $N(\boldsymbol{k})$, which is related to the wave height spectrum, $\Psi(\boldsymbol{k})$, and the degree of saturation, $B(\boldsymbol{k})$, by

$$N(\boldsymbol{k}) = \frac{g}{\sigma}\Psi(\boldsymbol{k}) = \frac{g}{\sigma}k^{-4}B(\boldsymbol{k}) \tag{1.4}$$

for surface gravity waves. The wave action density then evolves according to

$$\frac{\mathrm{d}N}{\mathrm{d}t} = -\nabla_k \cdot T(\boldsymbol{k}) + S_w - D, \tag{1.5}$$

where S_w is the wind input, $T(\boldsymbol{k})$ is the flux of the wave action by nonlinear wave interactions (∇_k is the gradient operator in $\boldsymbol{k}$) and D is the dissipation due to wave breaking. Within the equilibrium range, the sum of the three forcing terms must vanish. Kitaigorodskii (1983) developed a model that follows from the work of Hasselmann *et al.* (1973) and Zakharov & Filonenko (1966) in assuming that within the equilibrium range both the wind input and the dissipation are negligible. Then, the nonlinear flux divergence must also vanish to maintain the equilibrium. This assumption led to a form of the frequency spectrum that is proportional to σ^{-4}.

Phillips (1985) argued that (i) wind-wave generation models suggest that the energy transfer from wind to waves increases with wavenumber and thus cannot be neglected at the high wavenumbers in the equilibrium range, and (ii) breaking waves occur at all scales leading to dissipation of wave action at all wavenumbers. Hence, Phillips (1985) argued that in the equilibrium range the three input terms to the wave action conservation equation are all of the same order of magnitude and balance one another. He further assumed, following Kitaigorodskii (1983), that, in the equilibrium range, the divergence of the wave action flux is proportional to the cube of the local degree of saturation

$$-\nabla_k \cdot T(\boldsymbol{k}) \propto gk^{-4}B^3(\boldsymbol{k}), \tag{1.6}$$

and that the form of the wind input term is

$$S_w = \beta_g(\boldsymbol{k})N(\boldsymbol{k}) = \beta_g(\boldsymbol{k})\frac{g}{\sigma}k^{-4}B(\boldsymbol{k}), \tag{1.7}$$

where the wave growth rate, following Plant (1982), is

$$\beta_g(k,\theta) = c_\beta \sigma \frac{\rho_a u_*^2}{\rho_w c^2}\cos^{2p}(\theta). \tag{1.8}$$

It follows that the nonlinear interaction term (1.6) and the wind input term (1.7) are proportional to each other, and that the equilibrium degree of saturation is

$$B(k,\theta) = \beta\cos^p(\theta)\frac{u_*}{c} = \beta\cos^p(\theta)u_* g^{-1/2}k^{1/2}. \tag{1.9}$$

Here, c is the phase speed of waves, c_β, p and β are empirical coefficients, which Phillips took to be constants, and ρ_a and ρ_w are densities of air and water, respectively. The linear dispersion relation has been used to obtain the final form. Hence, according to this model, $B(k)$ is proportional to $k^{1/2}$ and u_*. If the wavenumber and frequency are related through the linear dispersion relation then Phillips showed that the frequency spectrum takes the form

$$\Phi(\sigma) = \alpha_p u_* g\sigma^{-4}, \tag{1.10}$$

(α_p is an empirical constant) which is consistent with the form (1.2) proposed by Toba (1973). We note that (1.9) is not consistent with the data of Banner *et al.* (1989).

Phillips' (1985) model enjoys success, but the model is based on the assumption that the surface wave field is a superposition of small-amplitude sinusoidal waves. Therefore, it is not likely to be applicable at very high winds when breaking waves are prevalent. Belcher & Vassilicos (1997) proposed a model with sharp-crested breaking waves dominating the equilibrium range of the spectra. Their model is based on both kinematic and dynamical assumptions. The kinematic assumptions are that breaking

waves are sharp crested (so that slope is discontinuous at the crest) and that their shape is self-similar regardless of their scale. This assumption of self-similarity implies that the statistical properties of the breaking waves vary with the scale of the breaking waves as a power law. Their dynamical assumption is similar to that of Phillips (1985). The combination of these assumptions leads to an equilibrium wave spectrum of the form

$$\Psi(k,\theta) = \tfrac{1}{2}(2\pi)^{3/2}(\alpha_\Lambda\beta_\Lambda)^2 A_0 \Theta(\theta) k^{-4}, \tag{1.11}$$

where α_Λ, β_Λ and A_0 are coefficients, and $\Theta(\theta)$ is the angular distribution of breaking wave crests.

Their study also predicts a frequency spectrum in the form of

$$\Phi(\sigma) = 2\alpha_\Lambda^2\beta_\Lambda^2 \nu A_0 c_0 g \sigma^{-4}. \tag{1.12}$$

Here, c_0 is the phase speed of the largest breaking waves and ν is a constant. It is noteworthy that their wavenumber spectrum (proportional to k^{-4}) and their frequency spectrum (proportional to σ^{-4}) cannot be obtained with the linear dispersion relation between k and σ. This is explained by their model because, as the wavenumber k increases, the wavenumber spectrum receives contributions from smaller and smaller breaking waves, whereas the frequency spectrum is dominated through the whole of the equilibrium range by the bound harmonics of the largest breaking waves.

The two models reviewed here can be considered as two extremes. Phillips (1985) (and all earlier works) assumes that all waves are freely propagating sine waves of small amplitude. Therefore, we expect this model to be valid at the weak wind limit. On the other hand, Belcher & Vassilicos (1997) assume that all waves are sharp-crested breaking waves; an assumption that we expect to be valid only at the strong wind limit. Since the two models predict different forms of the wavenumber spectrum, i.e. $k^{-7/2}$ by Phillips (1985) and k^{-4} by Belcher & Vassilicos (1997), the question arises as to whether there is a smooth transition between the two. And if there is, what parameters determine when and where this transition takes place? The aim of this paper is to answer these questions.

1.3. *Momentum budget in the equilibrium range*

It is known that, particularly in high winds, surface waves support a major part of the total wind stress through the form drag at higher wavenumbers (e.g. Banner & Peirson 1998). Therefore, the waves in the equilibrium range are expected to support a significant portion of the total wind stress. It is then of interest to consider the total budget of momentum and, in particular, the relation between the total momentum flux from wind and the momentum flux into the waves.

Consider the momentum budget of the model of Phillips (1985). Using his model results, we examine the wind stress supported by a particular wave component within the equilibrium range. Following, for example, Makin, Kudryavtsev & Mastenbroek (1995), the component of the stress in the mean wind direction supported by wavenumbers between $\boldsymbol{k}$ and $\boldsymbol{k} + d\boldsymbol{k}$, namely $\mathrm{d}\tau_w$, is expressed as

$$\mathrm{d}\tau_w = \beta_g(k,\theta)\rho_w\sigma\Psi(\boldsymbol{k})\cos\theta\,\mathrm{d}\boldsymbol{k} = c_\beta\beta\rho_a u_*^3 g^{-1/2}k^{-3/2}\cos^{3p+1}(\theta)\,\mathrm{d}\boldsymbol{k}, \tag{1.13}$$

using (1.8) and (1.9). Hence, the momentum flux is proportional to u_*^3. On the other hand, the total wind stress is proportional to u_*^2 by definition. This means that as the wind friction velocity u_* increases, the same wave component must support an increasing proportion of the total stress. Since the equilibrium range itself generally widens as the wind speed increases, the momentum flux into the waves in the

entire equilibrium range increases faster than u_*^3. Thus, the model of Phillips (1985) must break down beyond a critical wind stress because it violates conservation of momentum: the momentum flux into the equilibrium range exceeds the stress supplied by the wind. Clearly, momentum conservation adds an additional constraint which is especially important at high wind speeds. The formulation of this constraint and its consequences are the subject of this paper.

1.4. *A new model of the equilibrium range*

We use here new understanding of wind forcing of waves to develop an analytical model of the equilibrium range that satisfies overall momentum conservation. The key ingredient of our model is the effect of *sheltering*, whereby waves remove momentum from wind thus leaving a smaller stress to force growth of the shorter waves. This idea of sheltering was introduced by Janssen (1982) and discussed by Janssen (1989, 1991) and Jenkins (1992) in the context of numerical wave forecast models. This process was incorporated into a model of the roughness of the sea surface developed by Makin *et al.* (1995) and Makin & Kudryavtsev (1999). Kudryavtsev, Makin & Chapron (1999) develop a sophisticated model for short-gravity and capillary waves that accounts for sheltering. Their focus was the capillary waves and so their model also parameterizes many other processes, which meant their model required numerical solution. Here, we focus on the gravity waves in the equilibrium range. The resulting model is then amenable to analytical solution, which leads to fresh insights into the role of sheltering.

Evidence of the sheltering effect has recently been reported by Chen & Belcher (2000), who show that wind-forced growth of short wind waves in the presence of a long paddle-generated wave is reduced by sheltering by the paddle wave. In addition, Makin & Kudryavtsev (1999) and Belcher (1999) show how the concept of waves sheltering themselves yields a nonlinear correction to the growth rate that agrees with computations. These studies offer evidence that the concept of sheltering can be quantified reliably.

In this study, we focus on the components of the wind sea that propagate as nearly linear waves, and which therefore can be treated as a superposition of propagating sinusoidal waves. The contribution to the spectrum from highly nonlinear waves that are breaking is considered in a companion paper (Belcher & Hara 2002). Hence, in § 2 of this paper, following Markin *et al.* (1995), we apply the idea of sheltering to a spectrum of waves, which constrains overall momentum to be conserved. Following Phillips (1985), in § 3 a dynamical balance is imposed between the wind input, the nonlinear wave interaction, and dissipation by breaking for waves in the equilibrium range. This yields a new analytical form of the equilibrium spectrum associated with freely propagating sinusoidal water waves. The model is compared with previous observations of both the wavenumber spectrum and the frequency spectrum in § 4. Finally, in § 5 the results are summarized and there is further discussion.

2. Wind forcing in a spectrum of waves

Consider waves generated by a steady uni-directional wind, so that the wave spectrum is symmetric about the wind direction $\theta = 0$. Then, following Makin *et al.* (1995), the total wind stress τ_{tot} is expressed as the sum of the wave induced stress τ_w and the turbulent stress τ_t,

$$\tau_{tot}(z) = \rho_a u_*^2 = \tau_w(z) + \tau_t(z), \tag{2.1}$$

and all three components of the stress are collinear. Here, z is a vertical coordinate measured (upward) from the instantaneous water surface. Very close to the water surface, within the viscous sublayer, there is also a viscous contribution to the stress. Since the depth of the viscous sublayer is so much smaller than the scale of waves considered in this study, $\tau_t(z = 0)$, the turbulent stress just above the viscous layer, is equal to the stress supported by viscosity actually at the water surface and so the viscous stress does not need to be considered explicitly (Belcher, Harris & Street 1994). If the waves were generated by winds with non-uniform directions, then the three components of the stress in (2.1) would have to be treated as vector quantities. Such conditions are not considered further here.

Under stationary and homogeneous conditions the total wind stress τ_{tot} (and the friction velocity u_* defined such that $\tau_{tot} = \rho_a u_*^2$) is constant with height in the lower part of the atmospheric boundary layer. However, both τ_w and τ_t vary with height. If the surface waves have low slope and propagate according to the linear dispersion relation, then the total wave-induced stress caused by the spectrum of waves is just the sum of the contributions from each Fourier wave component. Hence, according to Makin *et al.* (1995), the wave-induced stress actually at the surface becomes

$$\tau_w(0) = \int_0^\infty \int_{-\pi/2}^{\pi/2} \beta_g(k,\theta)\rho_w \sigma \Psi(k,\theta) \cos\theta \, \mathrm{d}\theta \, k \, \mathrm{d}k. \tag{2.2}$$

(The contribution to the wave-induced stress from waves propagating against wind $|\theta| > \frac{1}{2}\pi$ is negligible because the energy in these components is so small. Therefore, the integration in θ spans $-\frac{1}{2}\pi$ to $\frac{1}{2}\pi$ only.)

According to the analysis of Belcher & Hunt (1993) the wave induced stress, τ_w, associated with waves of wavenumber k decays across the inner region, which has depth $L(k)$, with $kL \ll 1$. Makin *et al.* (1995) and Makin & Kudryavtsev (1999) therefore introduce a function $F(k,z)$ of the wave-induced stress to represent this decay such that

$$F(k,z) = 1(z = 0), \quad F(k,z) = 0 \quad (z \gg L(k)). \tag{2.3}$$

The wave-induced stress due to a spectrum of waves then varies with height according to

$$\tau_w(z) = \int_0^\infty \int_{-\pi/2}^{\pi/2} \beta_g(k,\theta)\rho_w \sigma \Psi(k,\theta) F(k,z) \cos\theta \, \mathrm{d}\theta \, k \, \mathrm{d}k. \tag{2.4}$$

Belcher & Hunt (1993) show that the growth rate $\beta_g(k,\theta)$ of a particular wave scale is determined primarily by the turbulent stress inside the corresponding inner region. In addition Belcher (1999) and Makin & Kudryavtsev (1999) show that the growth rate is determined by the local turbulent stress, denoted by $\tau_t^l(k) = \rho_a[u_*^l(k)]^2$. Here, following Makin *et al.* (1995), we take this to be the turbulent stress τ_t evaluated at the height comparable to the depth of the inner region, i.e.

$$\begin{aligned} \tau_t^l(k) &= \tau_t(z = L^-(k)) \\ &= \tau_{tot} - \tau_w(z = L^-(k)) \\ &= \tau_{tot} - \int_0^\infty \int_{-\pi/2}^{\pi/2} \beta_g(k',\theta)\rho_w \sigma \Psi(k',\theta) F(k', z = L^-(k)) \cos\theta \, \mathrm{d}\theta \, k' \, \mathrm{d}k', \end{aligned} \tag{2.5}$$

where $z = L^-$ is evaluated just below $z = L$. Makin *et al.* (1995) show that sufficiently accurate results are obtained if the decay function $F(k,z)$ is approximated by a step

function, namely

$$F(k,z) = 1(z \leqslant L(k)), \quad F(k,z) = 0 \quad (z > L(k)). \tag{2.6}$$

The local turbulent stress then becomes

$$\begin{aligned}\tau_t^l(k) &= \tau_{tot} - \int_0^k \int_{-\pi/2}^{\pi/2} \beta_g(k',\theta)\rho_w \sigma \Psi(k',\theta)\cos\theta \,\mathrm{d}\theta\, k' \,\mathrm{d}k' \\ &= \tau_t(0) + \int_k^\infty \int_{-\pi/2}^{\pi/2} \beta_g(k',\theta)\rho_w \sigma \Psi(k',\theta)\cos\theta \,\mathrm{d}\theta\, k' \,\mathrm{d}k'. \end{aligned} \tag{2.7}$$

Hence, the local value of the turbulent stress, which acts to make waves of wavenumber k grow, is the total stress minus the wave-induced stress associated with waves with wavenumber smaller than k.

Following Makin & Mastenbroek (1996), Belcher (1999) and Makin & Kudryavtsev (1999) the growth rate, β_g, of waves of wavenumber k is then

$$\beta_g(k,\theta) = c_\beta \sigma \frac{\rho_a [u_*^l(k)]^2}{\rho_w c^2} h(\theta). \tag{2.8}$$

Phillips (1985) used a similar form for the growth rate (see his equation 1.8), but he used τ_{tot} in place of $\rho_a[u_*^l(k)]^2$, which leads to his results violating overall momentum conservation, as explained in § 1.3. When the reduced local stress is correctly used in the formula for wave growth, then momentum is conserved overall.

3. Determination of the wave spectrum in the equilibrium range

For definiteness, suppose that the equilibrium range is established for wavenumbers in the range $k_0 < k < k_1$. For waves in the equilibrium range, the local turbulent stress obtained from (2.7) rewritten in terms of the saturation spectrum is

$$\begin{aligned}\rho_a[u_*^l(k)]^2 &= \rho_a[u_{*1}]^2 + \int_k^{k_1} \int_{-\pi/2}^{\pi/2} \beta_g(k',\theta)\rho_w \sigma k'^{-4} B(k',\theta)\cos\theta \,\mathrm{d}\theta\, k' \,\mathrm{d}k' \\ &= \rho_a[u_{*0}]^2 - \int_{k_0}^k \int_{-\pi/2}^{\pi/2} \beta_g(k',\theta)\rho_w \sigma k'^{-4} B(k',\theta)\cos\theta \,\mathrm{d}\theta\, k' \,\mathrm{d}k' \end{aligned} \tag{3.1}$$

(cf. Makin & Kudryavtsev 1999). Here, $\rho_a[u_{*0}]^2$ is the total stress minus the wave-induced stress supported by wavenumbers below k_0, and $\rho_a[u_{*1}]^2$ is the sum of the viscous stress (turbulent stress just outside the viscous sublayer) and the wave-induced stress supported by wavenumbers above k_1.

Following Phillips (1985), we assume that in the equilibrium range of the wavenumber spectrum the three sources in the wave action equation, (1.5), are in balance and are proportional to one another:

$$-\nabla_k \cdot T(\boldsymbol{k}) + S_w - D = 0 \quad \text{with} \quad |\nabla_k \cdot T(\boldsymbol{k})| \propto |S_w| \propto |D|. \tag{3.2}$$

This assumption is discussed further in § 3.4. The gain of energy by resonant wave–wave interactions at a particular wavelength is proportional to the cube of the resonantly interacting waves, and so it is further assumed, again following Kitaigorodskii (1983) and Phillips (1985), that the divergence of the wave action flux associated with resonant wave–wave interactions scales in the equilibrium range as the cube of the local degree of saturation, $B(\boldsymbol{k})$, namely

$$-\nabla_k \cdot T(\boldsymbol{k}) = \alpha' g k^{-4} B^3(\boldsymbol{k}), \tag{3.3}$$

where α' is a dimensionless coefficient. Then, the proportionality of the three forcing terms allows us to set

$$S_w = \alpha g k^{-4} B^3(\boldsymbol{k}), \tag{3.4}$$

$$-D = \alpha'' g k^{-4} B^3(\boldsymbol{k}), \tag{3.5}$$

where α and α'' are dimensionless coefficients, whose magnitude is comparable to that of α, and satisfy

$$\alpha + \alpha' + \alpha'' = 0. \tag{3.6}$$

In the subsequent analysis, we will determine the coefficient α and hence also an explicit expression for the wind input term. However, the coefficients α' and α'' will not need to be determined to calculate the spectra. Hence, complete solutions for the nonlinear transfer and dissipation will not be found here.

Since the wind input of wave action is written

$$S_w = \beta_g(\boldsymbol{k}) g^{1/2} k^{-9/2} B(\boldsymbol{k}), \tag{3.7}$$

it follows from (3.4) that

$$\beta_g(\boldsymbol{k}) g^{1/2} k^{-9/2} B(\boldsymbol{k}) = \alpha g k^{-4} B^3(\boldsymbol{k}), \tag{3.8}$$

and the saturation spectrum in the equilibrium range takes the form

$$B(\boldsymbol{k}) = \left[\alpha^{-1} \beta_g(\boldsymbol{k}) g^{-1/2} k^{-1/2}\right]^{1/2}. \tag{3.9}$$

This solution shows a resemblance to the solution obtained by Kudryavtsev *et al.* (1999) in their equation (44). However, their solution was obtained from a different dynamical balance, and contains an empirical constant, α_g. Here, in contrast, α is a coefficient that is independent of k, which, as shown in § 4, is determined from the external conditions by the constraint that overall momentum is conserved.

Equation (3.9) gives the saturation in terms of the growth rate, β_g, which in turn depends on u_*^l and hence on k. To find the variation of $B(\boldsymbol{k})$ with k it is therefore necessary to calculate the variation of u_*^l with k. This is done next.

3.1. *Calculation of the local turbulent stress*

If (2.8) and (3.9) are substituted into the equation for overall momentum conservation, (3.1), then

$$\begin{aligned}[u_*^l(k)]^2 &= [u_{*1}]^2 + \int_k^{k_1} \left(\frac{\rho_a}{\rho_w}\right)^{1/2} {c_\beta}^{3/2} \alpha^{-1/2} c_\theta [u_*^l(k')]^3 g^{-1/2} k'^{-1/2} \, \mathrm{d}k' \\ &= [u_{*0}]^2 - \int_{k_0}^{k} \left(\frac{\rho_a}{\rho_w}\right)^{1/2} {c_\beta}^{3/2} \alpha^{-1/2} c_\theta [u_*^l(k')]^3 g^{-1/2} k'^{-1/2} \, \mathrm{d}k', \end{aligned} \tag{3.10}$$

where

$$c_\theta = \int_{-\pi/2}^{\pi/2} [h(\theta)]^{3/2} \cos\theta \, \mathrm{d}\theta. \tag{3.11}$$

Equation (3.10) is an integral equation for $u_*^l(k)$, which can be solved analytically by first differentiating with respect to k

$$2u_*^l \frac{\mathrm{d}u_*^l}{\mathrm{d}k} = -c_1 (u_*^l)^3 k^{-1/2}, \tag{3.12}$$

where

$$c_1 = \left(\frac{\rho_a}{\rho_w}\right)^{1/2} {c_\beta}^{3/2} \alpha^{-1/2} c_\theta g^{-1/2}. \tag{3.13}$$

The solution is

$$u_*^l = (c_1 k^{1/2} + c_2)^{-1} \tag{3.14}$$

where c_2 is the integration constant that is independent of k. If this solution is substituted into (3.10), the two constants are found to be related to stress partition across the equilibrium range by

$$c_1 = \left(\frac{1}{u_{*1}} - \frac{1}{u_{*0}}\right)\left(k_1^{1/2} - k_0^{1/2}\right)^{-1}, \tag{3.15}$$

$$c_2 = \left(-\frac{k_0^{1/2}}{u_{*1}} + \frac{k_1^{1/2}}{u_{*0}}\right)\left(k_1^{1/2} - k_0^{1/2}\right)^{-1}. \tag{3.16}$$

Here, the coefficients c_1 and c_2 are both positive for realistic oceanic conditions, as shown in the next section. The solution is written more economically on definition of the *sheltering wavenumber*, namely

$$k_s^{1/2} = \frac{c_2}{c_1} = \frac{-k_0^{1/2} u_{*0} + k_1^{1/2} u_{*1}}{u_{*0} - u_{*1}}. \tag{3.17}$$

The local friction velocity can then be written

$$u_*^l(k) = \frac{2u_{*s}}{1 + \left(k/k_s\right)^{1/2}}, \tag{3.18}$$

where the local friction velocity at the sheltering wavenumber is given by

$$u_{*s} = \frac{\left(k_1^{1/2} - k_0^{1/2}\right) u_{*1} u_{*0}}{2\left(k_1^{1/2} u_{*1} - k_0^{1/2} u_{*0}\right)}. \tag{3.19}$$

The sheltering wavenumber, k_s, represents the wavenumber at which the local friction velocity begins to be affected by sheltering by the longer wavelength waves. The value of k_s is uniquely determined once the wavenumber range of the equilibrium region is established, i.e. once k_0, k_1 and the ratio u_{*1}/u_{*0} are specified. Some practical estimates are made in the next section.

Figure 1 shows the variation of $u_*^l(k)$, normalized on u_{*s}, with normalized wavenumber k/k_s. This figure illustrates how the local friction velocity decreases as the wavenumber increases. For $k \ll k_s$, u_*^l asymptotically approaches a constant ($= 2u_{*s}$), i.e. waves in this wavenumber range support only a small portion of the total wind stress. On the other hand, for $k \gg k_s$ u_*^l decreases as $k^{-1/2}$, i.e. the waves of smaller wavenumbers are significantly affected by sheltering.

3.2. *The saturation spectrum*

Now that the variation of the local friction velocity with k has been obtained, return to calculation of the saturation spectrum, $B(k)$. The dimensionless coefficient α, originally defined in (3.4), is uniquely determined from (3.13) and (3.15):

$$\alpha = 4\frac{\rho_a}{\rho_w} c_\beta^3 c_\theta^2 \left(\frac{u_{*s}}{c_s}\right)^2, \tag{3.20}$$

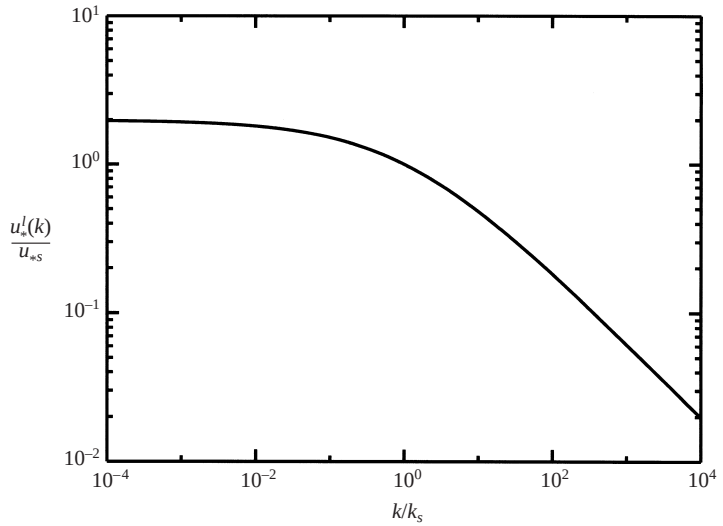

FIGURE 1. Normalized local friction velocity $u_*^l(k)/u_{*s}$ versus k/k_s.

where $c_s = (g/k_s)^{1/2}$. Introducing (3.18), (3.20) and (2.8) into (3.9), we obtain the degree of saturation

$$B(k,\theta) = \frac{1}{c_\beta c_\theta}\left[1 + \left(\frac{k_s}{k}\right)^{1/2}\right]^{-1} h(\theta)^{1/2}. \tag{3.21}$$

Hence, $B(\boldsymbol{k})$ is completely determined. We have been able to determine the magnitude of $B(\boldsymbol{k})$ because α is completely determined by the constraint that total momentum is conserved. In contrast, Phillips (1985) did not impose this constraint and so his expression for the degree of saturation contains an unknown multiplicative factor.

Integrating the saturation spectrum over all angles, the omni-directional degree of saturation is obtained:

$$B(k) = \frac{1}{c_\beta c'_\theta}\left[1 + \left(\frac{k_s}{k}\right)^{1/2}\right]^{-1}, \tag{3.22}$$

where

$$\frac{1}{c'_\theta} = \frac{1}{c_\theta}\int_{-\pi/2}^{\pi/2} h(\theta)^{1/2}\,\mathrm{d}\theta = \frac{\displaystyle\int_{-\pi/2}^{\pi/2} h(\theta)^{1/2}\,\mathrm{d}\theta}{\displaystyle\int_{-\pi/2}^{\pi/2} h(\theta)^{3/2}\cos\theta\,\mathrm{d}\theta}. \tag{3.23}$$

Notice how $B(k)$ depends on only three parameters, c_β, c'_θ and k_s. The first two come from the parameterization of the wind-induced growth rate (2.8), whereas k_s is determined by the extent of the equilibrium range (k_0 and k_1) and the stress partition, expressed in the ratio u_{*1}/u_{*0}. It is particularly noteworthy that $B(k)$ does not explicitly depend on the total wind stress, $\rho_a u_*^2$. Instead, it is determined by how the total wind stress is partitioned into three contributions, namely: the wave-induced stress supported by waves in the peak of the wave spectrum $k < k_0$; the wave-induced stress supported by waves in the equilibrium range ($k_0 < k < k_1$); the remaining stress

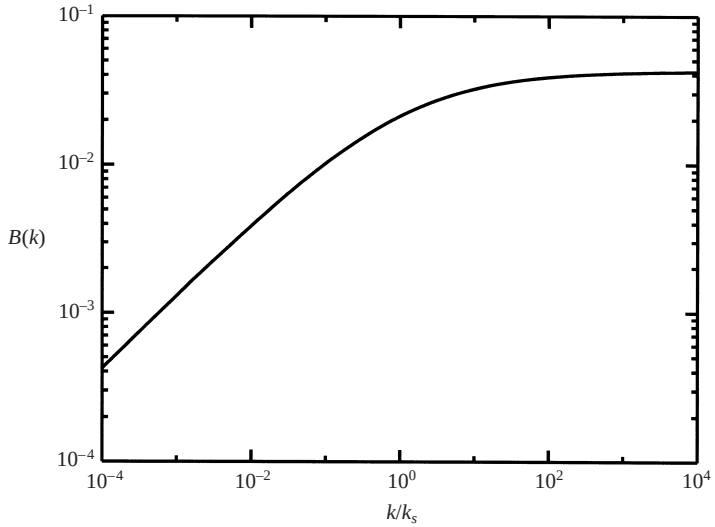

FIGURE 2. Degree of saturation $B(k)$ versus k/k_s.

that is the sum of the wave-induced stress supported by very short waves $k > k_1$ and the viscous stress.

Figure 2 shows $B(k)$ versus k/k_s. Here, we have set $c_\beta = 40$ after Plant (1982) and $c'_\theta = \frac{3}{16}\pi$ corresponding to $h(\theta) = \cos^2\theta$. There are two asymptotic limits of $B(k)$. First, if $k \ll k_s$,

$$B(k) \sim \frac{1}{c_\beta c'_\theta}\left(\frac{k}{k_s}\right)^{1/2}, \tag{3.24}$$

which has the dependence on k obtained by Phillips (1985). This agreement is to be expected because u^l_* is almost constant in this range, and so the growth rate used here relaxes to the same form as used by Phillips (1985). The saturation spectrum, $B(k)$, calculated here is, however, an improvement over the formula calculated by Phillips (1985) because our model gives the absolute magnitude of $B(k)$.

Secondly, in the limit $k \gg k_s$,

$$B(k) \sim \frac{1}{c_\beta c'_\theta}, \tag{3.25}$$

and so $B(k)$ is independent of wavenumber. This result is consistent with Belcher & Vassilicos (1997) who have also predicted that $B(k)$ is independent of k, albeit from very different arguments.

It is of interest to examine how our model result of $B(k)$ depends on the directional spreading of the wavenumber spectrum. If the directionality of the growth rate $h(\theta)$ (or the directionality of the resulting spectrum $h(\theta)^{1/2}$) is independent of k throughout the equilibrium range, the result is simply modified by a constant factor c'_θ for different choices of $h(\theta)$. Donelan *et al.* (1985) find that the directional spreading is roughly independent of frequency and is best parameterized by $\mathrm{sech}^2(1.24\theta)$ at frequencies above 1.6 times the peak frequency, which thus includes the equilibrium range. This function falls roughly between $\cos\theta$ and $\cos^3\theta$. If $h(\theta)$ is chosen to be $\cos^2\theta$, $\cos^4\theta$ and $\cos^6\theta$, corresponding to the directional spreading of the wavenumber spectrum of $\cos\theta$, $\cos^2\theta$ and $\cos^3\theta$, c'_θ is calculated to be $3\pi/16 \cong 0.5890$, $64/35\pi \cong 0.5821$ and $189\pi/1024 \cong 0.5798$, respectively. Hence, our result of $B(k)$ is surprisingly insensitive

to the choice of $h(\theta)$. As the directional spreading becomes narrower, the overall level of $B(k,\theta)$ becomes higher to support the same amount of momentum. However, if $B(k,\theta)$ is integrated in all θ, the resulting $B(k)$ depends on the directional spreading very weakly since the narrowness of the directional spreading offsets the increased height of $B(k,\theta)$ during the integration. If the directional spreading of the spectrum varies with k over the equilibrium range, the integral equation (3.10) must be solved numerically. Such a case is examined in Appendix A. Again, the values of $B(k)$ are found to be surprisingly insensitive to the directional spreading (see figure 5).

The results of the model developed by Kudryavtsev *et al.* (1999) for short waves shown in their figure 3(*b*) appear to show the transition from $k^{1/2}$ to k^0 as k increases, which is thus qualitatively consistent with the present model. This agreement is encouraging since the model of Kudryavtsev *et al.* (1999) includes the effect of sheltering in wind forcing. The analytical model developed here has the advantage that the sheltering wavenumber emerges naturally as a key parameter, and hence the role of sheltering is clear.

3.3. *Frequency spectrum*

Consider now the corresponding frequency spectrum. To be consistent with the argument so far, each wavenumber component propagates at the phase speed determined by the linear dispersion relation,

$$c = \sigma/k = (g/k)^{1/2}. \tag{3.26}$$

Effects of mean currents and Doppler shift in the wave frequencies by the advection of shorter waves by the orbital motion of dominant waves are both neglected. The omnidirectional degree of saturation, given in (3.22), can be converted to the frequency spectrum using the definition that the frequency spectrum has the same energy in a frequency band as the wavenumber spectrum has in a wavenumber band, namely,

$$\Phi(\sigma)\mathrm{d}\sigma = \Psi(k)k\,\mathrm{d}k = B(k)k^{-3}\,\mathrm{d}k, \tag{3.27}$$

and the dispersion relation

$$\frac{\mathrm{d}\sigma}{\mathrm{d}k} = c_g = \tfrac{1}{2}c = \tfrac{1}{2}g^{1/2}k^{-1/2}. \tag{3.28}$$

This procedure yields the frequency spectrum:

$$\Phi(\sigma) = \frac{2}{c_\beta c'_\theta} g^2\sigma^{-5}\left[1+\left(\frac{\sigma_s}{\sigma}\right)\right]^{-1}, \tag{3.29}$$

where $\sigma_s = (gk_s)^{1/2}$. The frequency spectrum is therefore proportional to σ^{-4} for $\sigma \ll \sigma_s$, which, as expected, has the same variation as Phillips (1985), and is proportional to σ^{-5} for $\sigma \gg \sigma_s$. Again, it is noteworthy that the present approach yields explicit values for the coefficients in terms of measurable quantities.

3.4. *Discussion*

The solution for the spectra in the equilibrium range is now complete and it is useful to review some of the assumptions of the model. First, we have assumed that the sum of the three source terms in the action balance equation is zero in the equilibrium range. This assumption is strictly valid only if the spectrum is fully developed and the fetch is unlimited. In practice, however, the assumption is approximately valid, and a local equilibrium is formed, if the sum of the three forcing terms is much smaller than the magnitude of each forcing term, that is, if the natural time or space

scale of spectral growth due to wind forcing (or spectral decay due to breaking) is much smaller than the actual time or space scale of the spectral variation. The time scale for the wind forcing reduces rapidly as the wavenumber increases. Therefore, even if the spectrum near the peak is still developing, we expect there to be a high wavenumber range of the spectrum over which our theory is approximately applicable.

Secondly, we assumed following Phillips (1985) that the three terms in the action balance equation are proportional to one another. Phillips starts by assuming that all three terms in the balance are of comparable importance and then assumes that the equilibrium range is scale invariant, i.e. the only wavenumber scale in the equilibrium range is k itself. Belcher & Vassilicos (1997) show that this implies that each term in the action balance must vary with k as a simple power law, and hence the three terms are proportional to one another. Now, scale invariance means that there is no special wavenumber in the equilibrium range, but the model developed in § 3 does produce a special wavenumber, namely, the sheltering wavenumber k_s. Hence, it appears that the model does not produce a scale invariant solution. This finding calls into question the original motivation for taking the three source terms proportional to one another. However, in the limits of k/k_s becoming small and large (but still well within the equilibrium range) the solutions become scale invariant and the procedure is formally valid. In the absence of a better argument, we assume as a working hypothesis that this proportionality extends throughout the equilibrium range. The main justification offered now is in the comparison between the model and measurements.

4. Comparison with observations of mature seas

The saturation spectrum, $B(k)$, obtained in § 3 can be evaluated once the sheltering wavenumber k_s has been calculated. This requires information about the upper and lower wavenumber limits of the equilibrium range, namely k_0 and k_1, and also the wind stress partitioning, namely the ratio of u_{*1} to u_{*0}. Such information is not readily available from field observations, and so it is necessary to make further assumptions in order to compare the model with previous observations. Here, we use a simple model with the following two assumptions.

(i) Assume that the wind sea is mature so that it is near to an equilibrium with the local winds. In these situations, very low wavenumber waves travel faster than the wind and do not gain energy from the wind (Cohen & Belcher 1999). Hence, these waves do not support wave-induced stress. The cutoff occurs at $u_*/c = u_* k^{1/2}/g^{1/2} \approx 0.07$ (Plant 1982). We use this criterion to define $k_0 = 0.0049 g/u_*^2$. The wave-induced stress is then small for wavenumbers below k_0 and so the local stress at wavenumber k_0 is equal to the total wind stress.

(ii) The upper bound k_1 is simply set to the value $100\,\mathrm{rad\,m^{-1}}$. Previous observations by Jähne & Riemer (1990), Hara *et al.* (1998), and others and the modelling of Kudryavtsev *et al.* (1999) all show that the wavenumber spectrum behaves very differently above and below this wavenumber, suggesting that the effects of surface tension and/or viscosity become significant above this wavenumber. In addition, assume here that the wind stress supported by the gravity–capillary and capillary waves that have higher wavenumber $k > k_1$ is negligible. Then $\tau_t(0) = \rho_a [u_{*1}]^2$ which both equal the viscous stress at the surface, τ_v.

With these assumptions, the local friction velocity at the bounds of the equilibrium range can be written

$$\rho_a [u_{*0}]^2 = \tau_{tot} \equiv \rho_a c_d U_{10}^2, \quad \rho_a [u_{*1}]^2 = \tau_v \equiv \rho_a c_t U_{10}^2. \tag{4.1}$$

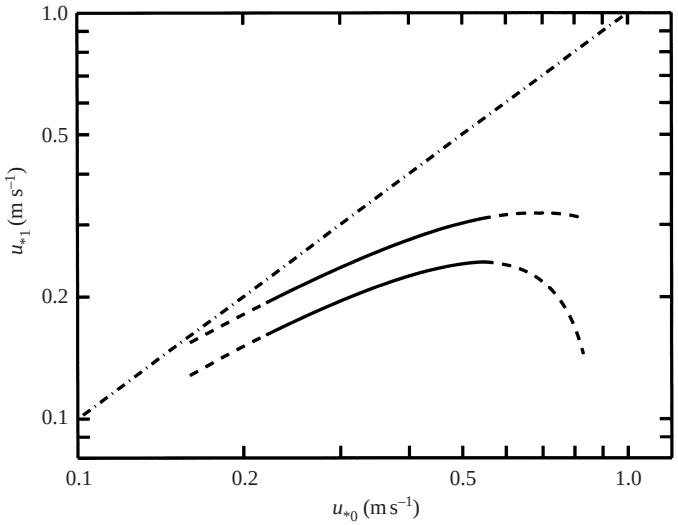

FIGURE 3. Relationship between u_{*0} and u_{*1} for mature seas. Solid and dashed lines indicate the upper and lower bounds based on Banner & Peirson (1998). Dashed lines indicate extended part of the estimates outside the wind speed range given by Banner & Peirson (1998). Dash-dot line corresponds to $u_{*0} = u_{*1}$.

The drag coefficients c_d and c_t are evaluated here using the correlations obtained recently by Banner & Peirson (1998), who measured both the total stress, τ_{tot}, and the stress supported by viscosity, τ_v. Based on both their own laboratory data and also field observations of mature waves, their best estimates were

$$c_d = (U_{10} \times 0.66 + 8 \pm 1) \times 10^{-4}, \quad c_t = (-U_{10} \times 0.5 + 11 \pm 1) \times 10^{-4}, \tag{4.2}$$

when U_{10} (the wind speed at 10 m above the mean sea level, measured in the unit of m s^{-1}) lay between 6 and 14. Note that Banner & Peirson (1998) gave upper and lower bounds of the drag coefficients rather than specific values for any given U_{10}.

By introducing (4.2) into (4.1), we may determine the possible range of the combination of (u_{*0}, u_{*1}) for a given U_{10}. By superposing such results for all U_{10}, we may determine the overall range of (u_{*0}, u_{*1}) allowed by the correlations of Banner & Peirson (1998), namely (4.2). Thus, the upper and lower bounds of u_{*1} are determined for a given u_{*0}. The results are shown in figure 3. Although (4.2) were obtained for $6 < U_{10} < 14\,\mathrm{m\,s^{-1}}$, the same form has been applied to the extended range of $4.5 < U_{10} < 19\,\mathrm{m\,s^{-1}}$, and the extensions are distinguished by dashed lines. It is evident that u_{*1} is smaller than u_{*0}, which shows that there is some sheltering at all values of u_{*0}. At lower wind stress, u_{*1} monotonically increases with u_{*0}. However, at high wind stress, u_{*1} ceases to increase and may even decrease with u_{*0}, suggesting that the sheltering effect becomes very strong.

We next calculate the upper and lower bounds of the sheltering wavenumber k_s for a given $u_* = u_{*0}$, using $k_0 = 0.0049g/u_*^2$, $k_1 = 100\,\mathrm{rad\,m^{-1}}$, as described above, and the values of u_{*1} for given u_{*0} from the upper and lower bounds of figure 3. The results are shown in figure 4. Clearly, k_s decreases monotonically as the wind friction velocity increases and the definition of k_s remains valid over the whole range of friction velocity examined (because the sign of c_2 in (3.16) remains positive). For $u_* < 0.5\,\mathrm{m\,s^{-1}}$, k_s is larger than $k_1 = 100\,\mathrm{rad\,m^{-1}}$ and so the sheltering is weak. Nevertheless, the value of k_s remains significant in determining the coefficients multiplying the spectra. For

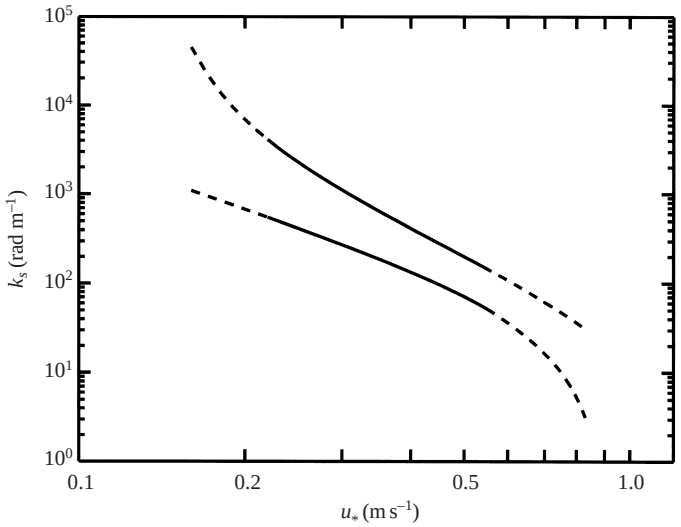

FIGURE 4. Upper and lower bounds of sheltering wavenumber k_s versus wind friction velocity u_*. Dashed lines indicate extended part of the estimates outside the wind speed range given by Banner & Peirson (1998).

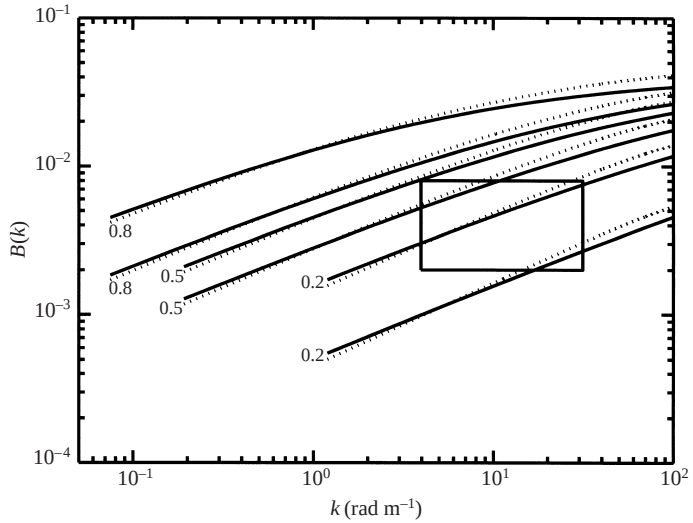

FIGURE 5. Upper and lower bounds of degree of saturation $B(k)$ versus k. Numbers on lines in the figure correspond to values of u_* in m s^{-1}. Hence, the two lines with the same number indicate the spread resulting from the spread in the correlation of Banner & Peirson (1998) used to evaluate the model. Dotted lines are the results with variable directional spreading (see Appendix A for details). The box indicates the range of data by Banner *et al.* (1989).

greater u_*, the sheltering becomes important and k_s becomes smaller. The uncertainty of k_s increases rapidly as the wind friction velocity decreases below 0.2 m s^{-1}, mainly because the wave-induced stress in the equilibrium range becomes small compared to the total wind stress and the stress supported by gravity–capillary waves, capillary waves and viscosity becomes increasingly important.

Figure 5 shows by solid lines the upper and lower bounds of $B(k)$ given by (3.20) versus k at three different wind friction velocities. At the lowest friction velocity

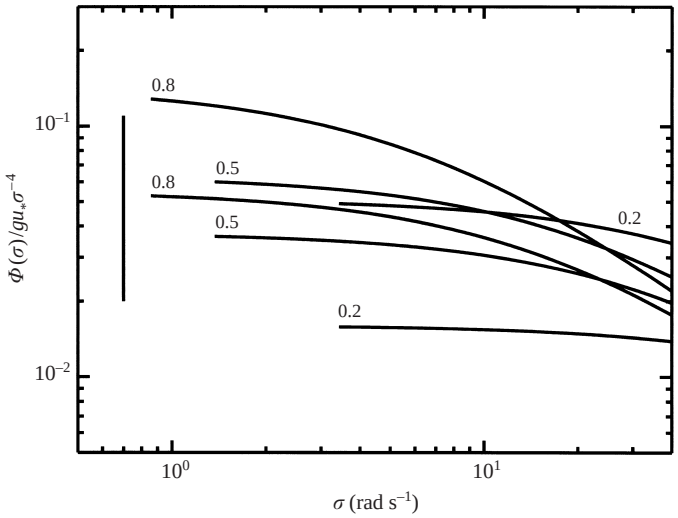

FIGURE 6. Upper and lower bounds of $\Phi(\sigma)/gu_*\sigma^{-4}$ versus σ. Numbers on lines correspond to values of u_* in m s^{-1}. Hence, the two lines with the same number indicate the spread resulting from the spread in the correlation of Banner & Peirson (1998) used to evaluate the model. The vertical line indicates the range given by Phillips (1985).

of 0.2 m s^{-1} where k_s is relatively large, $B(k)$ increases as $k^{1/2}$, consistent with the model by Phillips (1985). As the friction velocity increases and k_s decreases, the slope of $B(k)$ gradually decreases from $k^{1/2}$ to k^0 at higher wavenumbers. Therefore, it approaches the form of the equilibrium wavenumber spectrum suggested by Belcher & Vassilicos (1997). Banner *et al.* (1989) find from their measurements that $B(k)$ is almost independent of wavenumber and wind stress, when the wavenumber lies between $k = 4$ and 31 rad m^{-1} and for wind speeds between 7 and 13 m s^{-1} (so that the friction velocity lies between 0.17 and 0.44 m s^{-1}). Their data yield a value of $B(k)$ between 0.002 and 0.008 with the average value of about 0.004. We show the range of the degree of saturation observed by Banner *et al.* (1989) by a square box in figure 5. The values from the model are in agreement over the range of friction velocities observed, which is remarkable given the assumptions made to estimate u_{*1} in the model. The model does predict that $B(k)$ increases slightly with k and with u_*, so that once the friction velocity has reached 0.8 m s^{-1} the values of B are significantly higher than at 0.5 m s^{-1}. Clearly, further observations are required to validate these aspects of the model. Dotted lines in figure 5 are the results obtained numerically when the directional spreading varies with wavenumber, as discussed in Appendix A. It is clear that qualitatively the results are unchanged, and that even quantitatively the results change by only 15–20%.

Figure 6 shows the variation with σ of the upper and lower bounds of $\Phi(\sigma)/(gu_*\sigma^{-4})$ obtained from the present model for $u_* = 0.2$, 0.5 and 0.8 m s^{-1}. This form was chosen for plotting for two reasons. First, Phillips' (1985) model suggests that $\Phi(\sigma)/(gu_*\sigma^{-4}) = \alpha_p$, a constant, and so this plot indicates the differences between the present model and Phillips (1985). Secondly, Phillips (1985) shows that data then to hand were consistent with his form for frequencies not too much greater than the peak in the spectrum. The data yielded values of α_p in the range 0.02–0.11 (and 0.06–0.11 for most of the field observations). This range is marked on figure 6. Figure 6 shows that $\Phi(\sigma)$ varies nearly as σ^{-4} at lower frequencies and at low friction velocities, so that in this respect

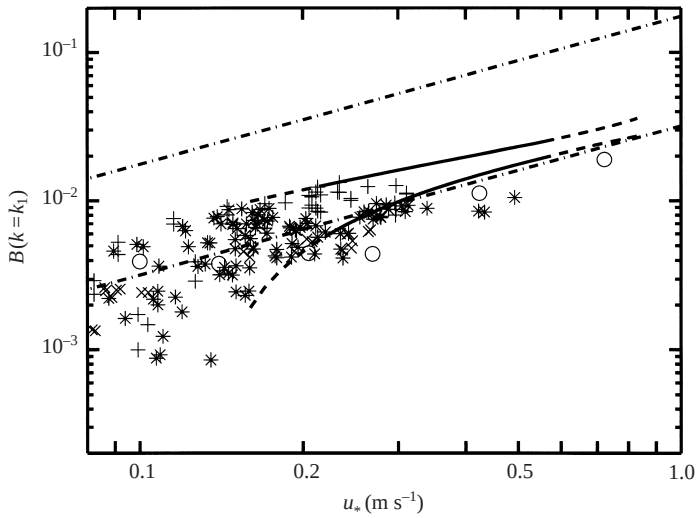

FIGURE 7. Degree of saturation $B(k)$ at $k = k_1 = 100\,\mathrm{rad\,m^{-1}}$ versus friction velocity u_*. Solid and dashed lines are upper and lower bounds estimated in this study. Dashed lines indicate extended part of the estimates outside the wind speed range given by Banner & Peirson (1998). Dash-dot lines are upper and lower bounds estimated by Phillips (1985), with the empirical coefficient α_p set to be between 0.02 and 0.11 based on comparison with observational data near the spectral peak. Observational data: ○, Jähne & Riemer (1990), in a wind wave tank; ∗, Hara *et al.* (1998), off California; +, Hara *et al.* (1998), off Cape Hatteras; ×, Hara *et al.* (1994), off Cape Cod.

the present model agrees with Phillips, as expected. In addition, the value obtained for $\Phi(\sigma)/(gu_*\sigma^{-4})$ from the present model lies within the range suggested by the data analysed by Phillips. At higher frequencies, and for stronger winds, the model curves deviate significantly downwards so that $\Phi(\sigma)$ approaches σ^{-5}. This tendency is in qualitative agreement with the tendencies found in the data of Forristall (1981).

As a final comparison with data, figure 7 shows the upper and lower bounds of the degree of saturation $B(k)$ at $k = k_1 = 100\,\mathrm{rad\,m^{-1}}$ versus the wind friction velocity u_*. Also shown are previous laboratory and field observations. In addition, the upper and lower bounds of the Phillips' (1985) spectrum are indicated by dash-dot lines, with the parameter α_p chosen to be 0.02–0.11 to match the field observations near the spectral peak. Since Phillips' (1985) spectrum decays more slowly with k than our model, if extended to $k = 100\,\mathrm{rad\,m^{-1}}$, his result becomes higher than our prediction.

The present model suggests that $B(k_1)$ monotonically increases with u_* in agreement with the data. Although the data do appear to lie slightly below the model at the higher u_*, the agreement is much improved compared to Phillips (1985) who significantly overestimates the high wavenumber end of the equilibrium spectrum. The uncertainty in the model is large below $u_* = 0.2\,\mathrm{m\,s^{-1}}$, because the correlations described above and used here for u_{*0} and u_{*1} have large uncertainty in this range. The observational data also scatter widely below $u_* = 0.2\,\mathrm{m\,s^{-1}}$. This is probably because at lower winds the stress supported by gravity–capillary waves, capillary waves, and viscosity becomes more important than the stress supported by gravity waves in the equilibrium range. Since the former varies widely at low winds because of its sensitivity to surfactants and other environmental conditions (e.g. Hara *et al.* 1998), it modifies the overall stress partitioning and increases the uncertainty of $B(k_1)$.

Overall, the agreement between the present model and observations for mature seas are good, particularly considering the assumptions introduced in determining k_0, k_1 and u_{*1}/u_{*0}.

5. Concluding remarks

We have developed a new analytical model for the equilibrium range of ocean wave spectra. This work was motivated by our observation that Phillips' (1985) model does not satisfy overall momentum conservation at high winds. The key element of the present model is the representation of the wind forcing, which is based on the idea, following Makin & Mastenbroek (1996), Makin & Kudryavtsev (1999) and Belcher (1999) that the wave growth rate at a particular wavenumber is determined not by the total wind stress, but by the local turbulent stress, which is the total wind stress reduced by the sheltering of longer waves.

This idea of sheltering, originally suggested by Janssen (1982), enforces total momentum conservation even at high winds, when a significant part of the wind stress is supported by waves in the equilibrium range.

This wind forcing representation is introduced to the dynamical framework for the equilibrium range set out in Phillips (1985), which requires the following approximations:

(i) The wave field is a superposition of linear waves.

(ii) The terms in the wave action equation representing wind forcing, nonlinear interaction and dissipation are all of the same order of magnitude and are proportional to one other.

(iii) The nonlinear interaction term is proportional to the cube of the local wave spectrum in the equilibrium range.

Combination of these assumptions yielded an integral equation for the local friction velocity, $u_*^l(k)$, which here was solved analytically. In particular, we identified the *sheltering wavenumber*, k_s, above which sheltering reduces the local turbulent stress, $u_*^l(k)$. The magnitude of k_s is determined by the range of wavenumbers in the equilibrium range and the partition of the stress across the range, expressed as u_{*1}/u_{*0}.

The model yields analytical formulae for degree of saturation, $B(k)$, and the frequency spectrum, $\Phi(\sigma)$, namely

$$B(k) = \frac{1}{c_\beta c'_\theta}\left[1 + \left(\frac{k_s}{k}\right)^{1/2}\right]^{-1}, \quad \Phi(\sigma) = \frac{2}{c_\beta c'_\theta} g^2 \sigma^{-5}\left[1 + \left(\frac{\sigma_s}{\sigma}\right)\right]^{-1}, \tag{5.1}$$

where $c_\beta \approx 40$ and $c'_\theta \approx 0.5$ are constants in the parameterization of the wave growth rate. In the limit of small wavenumber and frequency or low wind stress, so that $k \ll k_s$ and $\sigma \ll \sigma_s$, there is little sheltering. Then $B(k)$ varies as $k^{1/2}$ and $\Phi(\sigma)$ varies as σ^{-4}, just as in the model of Phillips (1985). However, the imposition of the additional constraint that momentum is conserved fixes the values of the coefficients multiplying these power laws, i.e. $B(k)$ and $\Phi(\sigma)$ are completely determined by the model. The coefficients vary nonlinearly with u_*, because they depend, through k_s and σ_s, on how stress is partitioned in the wave spectrum. At high wavenumbers and frequencies or high wind stress, so that $k \gg k_s$ and $\sigma \gg \sigma_s$, there is strong sheltering. Then $B(k)$ approaches a value that does not vary with wavenumber, which is consistent with the model of Belcher & Vassilicos (1997). This variation of $B(k)$ from $k^{1/2}$ to k^0 is consistent with the numerical results of Kudryavtsev *et al.* (1999). The variation of

the frequency spectrum $\Phi(\sigma)$ changes from σ^{-4} to σ^{-5}, a change that is seen in the observations of Forristall (1981).

Values of $B(k)$ and $\Phi(\sigma)$ have been evaluated from the model for mature seas using the recent observations of the stress partitioning by Banner & Peirson (1998). The results show encouraging agreement with previous field observations, particularly at high wavenumbers and wind speeds, when the model of Phillips (1985) tends to over-predict the spectral level.

The model yields the form of the wind input S_w to the wave action equation (1.5). The dissipation D is assumed to be proportional to S_w, and so the functional form of the dissipation is

$$D(\boldsymbol{k}) \propto gk^{-4}\left[1+\left(\frac{k_s}{k}\right)^{1/2}\right]^{-3} h(\theta)^{3/2}. \tag{5.2}$$

If we then follow the argument of Phillips (1985) to define the distribution function of breaking wave crests $\Lambda(\boldsymbol{c})$ such that $\Lambda(\boldsymbol{c})\,\mathrm{d}\boldsymbol{c}$ represents the average total length per unit surface area of breaking fronts that have velocities in the range $\boldsymbol{c}$ to $\boldsymbol{c}+\mathrm{d}\boldsymbol{c}$, and relate $D(\boldsymbol{k})$ with $\Lambda(\boldsymbol{c})$, we obtain

$$\Lambda(\boldsymbol{c}) \propto gc^{-4}\left(1+\frac{c}{c_s}\right)^{-3} h(\theta)^{3/2}. \tag{5.3}$$

In the limit of low wind or low wavenumbers, when $c \gg c_s$, we recover the result of Phillips (1985), i.e. $\Lambda(\boldsymbol{c})$ decreases like c^{-7}. However, at the high wind or high wavenumber limit, when $c \ll c_s$, $\Lambda(\boldsymbol{c})$ decreases more slowly, like c^{-4}. Hence, the present model suggests that the breaking crests of slower (shorter) waves are less frequent at high winds. Recent estimations of $\Lambda(\boldsymbol{c})$ based on observations of white-caps associated with short waves appear to be consistent with the model (Melville & Matusov 2002).

It is not currently possible to make quantitative comparisons between the model and observations of young growing seas, since neither the range of wavenumbers in the equilibrium range nor the partitioning of stress in a growing spectrum can be determined with sufficient accuracy. Nevertheless, qualitative estimates can be made. Banner & Peirson (1998) estimate that for a given U_{10} the drag coefficient c_d is larger for young seas than for mature seas while c_t remains similar. In addition, we expect the lower bound k_0 of the equilibrium range to be higher than the peak wavenumber in younger seas. Both tend to make k_s smaller in young seas. Then, the degree of saturation $B(k)$ is likely to be larger at a given value of k. This suggests an interesting possibility. This process may explain the observation that under steady wind forcing, the wave spectrum at a fixed wavenumber 'overshoots', i.e. it increases with fetch or wave age until a maximum value is attained and then decreases slightly before finally approaching the equilibrium state (Hasselmann *et al.* 1973). Further measurements of both the drag and the wavenumber spectrum are required to test these hypotheses.

The theory presented here is based on a set of assumptions. Perhaps the most questionable is the assumption, originally introduced by Phillips (1985), that the wind forcing, dissipation, and nonlinear interaction are of the same order of magnitude and balance one another over the equilibrium range. An alternative assumption, introduced by Zakharov & Filonenko (1966) and followed by Hasselmann *et al.* (1973) and Kitaigorodskii (1983), is that the nonlinear interactions alone dominate in the equilibrium range. Current observational and theoretical understanding is not

sufficient to determine which assumption is correct, since neither the nonlinear interaction term nor the dissipation term can be evaluated with confidence. Currently, the calculation of the nonlinear interaction term is based on the Boltzmann equation for four-wave interactions in wave prediction models. Although this approach is valid in the energy-containing range of the spectrum, it breaks down for interactions between very short waves and long waves (e.g. Komen *et al.* 1994). Therefore, it may well not be accurate in the equilibrium range. One possibility is a more direct numerical calculation of the nonlinear interactions, based, for example, on Zakharov's (1968) equation, which may yield better understanding of the role of nonlinear interactions in the equilibrium range. The evaluation of the dissipation term, on the other hand, will be possible only through further observational studies of breaking waves, since no theoretical framework exists to directly estimate the energy dissipation due to breaking waves. In any event, the present study has aimed to further develop the model proposed by Phillips (1985), which should help future efforts to distinguish between the two current approaches to modelling the equilibrium range.

T. H. would like to acknowledge the generous hospitality of the Department of Meteorology, University of Reading, where he was a visiting scientist and this work was initiated during the spring of 1999. T. H. also thanks University of Rhode Island for financial support during the visit. This work was, in part, supported by the NSF Grant OCE9458349 and the ONR Contract N00014-96-10542. S. E. B. is also grateful to the European Commission for financial support under grant ENV4-CT97-0460.

Appendix A

One of the assumptions of the present theory is that the three forcing terms are proportional at every wavenumber $\boldsymbol{k}$. This assumption then leads to the directional spreading of the spectrum being proportional to $h^{1/2}(\theta)$, where $h(\theta)$ is the directionality of the growth rate. In the bulk of the text it was assumed for mathematical simplicity that $h(\theta)$ remains independent of k throughout the equilibrium range. Here, we examine how our results are modified if we relax this assumption and allow the directional spreading to vary with k. Let us set

$$B(\boldsymbol{k}) = B(k) f(\theta; k), \tag{A 1}$$

with

$$\int_{-\pi/2}^{\pi/2} f(\theta; k)\, \mathrm{d}\theta = 1, \tag{A 2}$$

where $f(\theta; k)$ is the directional spreading function that may vary with k. Let us assume that the directionality of the growth rate $h(\theta)$ is independent of the directional spreading $f(\theta; k)$ and that the proportionality of the three forcing terms is applied only after each forcing term is integrated in all angles. Then, (3.8) is modified to

$$\int_{-\pi/2}^{\pi/2} \beta_g(\boldsymbol{k}) g^{1/2} k^{-9/2} B(\boldsymbol{k})\, \mathrm{d}\theta = \int_{-\pi/2}^{\pi/2} \alpha g k^{-4} B^3(\boldsymbol{k})\, \mathrm{d}\theta, \tag{A 3}$$

and $B(k)$ is related to u_*^l as

$$B(k) = \left[\frac{c_\beta}{\alpha} \frac{\rho_a}{\rho_w} \frac{k}{g} (u_*^l)^2 c_4(k) \right]^{1/2}, \tag{A 4}$$

with

$$c_4(k) = \frac{\int_{-\pi/2}^{\pi/2} hf \, \mathrm{d}\theta}{\int_{-\pi/2}^{\pi/2} f^3 \, \mathrm{d}\theta}. \tag{A 5}$$

It is straightforward to show on differentiation that the integral equation, (3.12), becomes

$$2u_*^l \frac{\mathrm{d}u_*^l}{\mathrm{d}k} = -c_1 (u_*^l)^3 k^{-1/2} c_5(k), \tag{A 6}$$

where

$$c_1 = \left(\frac{\rho_a}{\rho_w}\right)^{1/2} {c_\beta}^{3/2} \alpha^{-1/2} c_\theta g^{-1/2} \tag{A 7}$$

$$c_5(k) = \frac{\int_{-\pi/2}^{\pi/2} hf \cos\theta \, \mathrm{d}\theta}{\int_{-\pi/2}^{\pi/2} h^{3/2} \cos\theta \, \mathrm{d}\theta} (c_4(k))^{1/2}. \tag{A 8}$$

Therefore, the only modification to the integral equation is the coefficient $c_5(k)$ multiplied on the right-hand side. The coefficient c_5 is not very sensitive to the choice of the directional spreading function. For example, if we keep $h(\theta) = \cos^2\theta$ as before and set the directional spreading function as

$$f(\theta) = \frac{\cos^p \theta}{\int_{-\pi/2}^{\pi/2} \cos^p \theta \, \mathrm{d}\theta}, \tag{A 9}$$

and vary p from 0 to 2, the coefficient c_5 increases from 0.8003 at $p = 0$ (uniform directional spreading) to 1 at $p = 1$ (the original assumption), and then decreases slightly to 0.9918 at $p = 2$.

We now examine here how the results for the equilibrium spectrum of mature seas, presented in § 4, are modified if the directional spreading gradually widens with k through the equilibrium range. As discussed earlier, Donelan *et al.* (1985) report that directional spreading not far from the spectral peak can be described as $\mathrm{sech}^2(1.24\theta)$, which falls roughly between $\cos\theta$ and $\cos^3\theta$. We therefore choose a form for the spreading that is similar to Donelan *et al.* at low k and then broadens to the most extreme form, namely omni-directional at large k. The directional spreading function, (A 9), is then

$$p = 2\left(1 - \frac{\log k - \log k_0}{\log k_1 - \log k_0}\right). \tag{A 10}$$

Then, the spreading, f, at k_0 is proportional to $\cos^2\theta$, and at k_1 becomes independent of θ, so that the spreading is uniform around all angles. With this choice of $f(\theta; k)$ the integral equation, (A 6), is solved numerically for u_*^l with the same boundary conditions at k_0 and k_1 as in § 4. The result is then introduced to (A 4) to solve for $B(k)$. In figure 5 the results of $B(k)$ with this variable directional spreading are shown by dotted lines and are compared with the original results (solid lines) with fixed directional spreading. It is seen that the qualitative characteristics of the solutions are unchanged, that is, the solutions still exhibit transition from $k^{1/2}$ dependence at low

wavenumber/wind to k^0 dependence at high wavenumber/wind. The only noticeable quantitative difference is that $B(k)$ is increased by 15–20% at high k.

This calculation suggests that the analytical results, which assume that the spreading does not change with k are qualitatively unaffected and are only slightly modified quantitatively if the directional spreading does vary with k over the equilibrium range.

REFERENCES

Banner, M. L. 1990 Equilibrium spectra of wind waves. *J. Phys. Oceanogr.* **20**, 966–984.

Banner, M. L., Jones, I. S. F. & Trinder, J. C. 1989 Wavenumber spectra of gravity waves. *J. Fluid Mech.* **198**, 321–344.

Banner, M. L. & Peirson, W. L. 1998 Tangential stress beneath wind-driven air–water interfaces. *J. Fluid Mech.* **364**, 115–145.

Belcher, S. E. 1999 Wave growth by non-separated sheltering. *Eur. J. Mech.* B/*Fluids* **18**, 447–462.

Belcher, S. E. & Hara, T. 2002 The contribution of breaking waves to wind–wave spectra. *In preparation.*

Belcher, S. E., Harris, J. A. & Street, R. L. 1994 Linear dynamics of wind waves in coupled turbulent air–water flow. Part 1. Theory. *J. Fluid Mech.* **271**, 119–151.

Belcher, S. E. & Hunt, J. C. R. 1993 Turbulent shear flow over slowly moving waves. *J. Fluid Mech.* **251**, 109–148.

Belcher, S. E. & Vassilicos, J. C. 1997 Breaking waves and the equilibrium range of wind–wave spectra. *J. Fluid Mech.* **342**, 377–401.

Chen, G. & Belcher, S. E. 2000 Effects of long waves on wind-generated waves. *J. Phys. Oceanogr.* **30**, 2246–2256.

Cohen, J. E. & Belcher, S. E. 1999 Turbulent shear flow over fast-moving waves. *J. Fluid Mech.* **386**, 345–371.

Donelan, M. A., Hamilton, J. & Hui, W. H. 1985 Directional spectra of wind-generated waves. *Phil. Trans. R. Soc. Lond.* A **315**, 509–562.

Forristall, G. Z. 1981 Measurements of a saturated range in ocean wave spectra. *J. Geophys. Res.* **86**, 8075–8084.

Hara, T., Bock, E. J., Edson, J. B. & McGillis, W. R. 1998 Observations of short wind waves in coastal waters. *J. Phys. Oceanogr.* **28**, 1425–1438.

Hara, T., Bock, E. J. & Lyzenga, D. 1994 *In situ* measurements of capillary–gravity wave spectra using a scanning laser slope gauge and microwave radars. *J. Geophys. Res.* **99**, 12593–12602.

Hasselmann, K. *et al.* 1973 Measurements of wind wave growth and swell decay during the Joint North Sea Wave Project (jonswap). *Herausgegeben vom Deutsch-Hydrograph. Inst.* A, no. 12.

Jähne, B. K. & Riemer, K. S. 1990 Two-dimensional wave number spectra of small-scale water surface waves. *J. Geophys. Res.* **95**, 11531–11546.

Janssen, P. A. E. M. 1982 Quasilinear approximation for the spectrum of wind-generated water waves. *J. Fluid Mech.* **117**, 493–506.

Janssen, P. A. E. M. 1989 Wave-induced stress and the drag of air flow over sea waves. *J. Phys. Oceanogr.* **19**, 745–754.

Janssen, P. A. E. M. 1991 Quasi-linear theory of wind wave generation applied to wave forecasting. *J. Phys. Oceanogr.* **21**, 1631–1642.

Jenkins, A. D. 1992 A quasi-linear eddy-viscosity model for the flux of energy and momentum to waves, using conservation law equations in a curvilinear system. *J. Phys. Oceanogr.* **22**, 843–858.

Kitaigorodskii, S. A. 1983 On the theory of the equilibrium range in the spectrum of wind-generated gravity waves. *J. Phys. Oceanogr.* **13**, 816–827.

Kitaigorodskii, S. A., Krasitskii, V. P. & Zaslavskii, M. M. 1975 On Phillips' theory of equilibrium range in the spectra of wind-generated gravity waves. *J. Phys. Oceanogr.* **5**, 410–420.

Komen, G. J., Cavaleri, L., Donelan, M., Hasselmann, K., Hasselmann, S. & Janssen, P. A. E. M. 1994 *Dynamics and Modelling of Ocean Waves.* Cambridge University Press.

Kudryavtsev, V. N., Makin, V. K. & Chapron, B. 1999 Coupled sea surface–atmosphere model. 2. Spectrum of short wind waves. *J. Geophys. Res.* **104**, 7625–7639.

MAKIN, V. K. & KUDRYAVTSEV, V. N. 1999 Coupled sea surface–atmosphere model. 1. Wind over waves coupling. *J. Geophys. Res.* **104**, 7613–7623.

MAKIN, V. K., KUDRYAVTSEV, V. N. & MASTENBROEK, C. 1995 Drag of the sea surface. *Boundary Layer Meteorol.* **73**, 159–182.

MAKIN, V. K. & MASTENBROEK, C. 1996 Impact of waves on air-sea exchange of sensible heat and momentum. *Boundary-Layer Met.* **79**, 279–300.

MELVILLE, W. K. & MATUSOV, P. 2002 Distribution of breaking waves at the ocean surface. *Nature* **417**, 58–63.

PHILLIPS, O. M. 1977 *Dynamics of the Upper Ocean.* Cambridge University Press.

PHILLIPS, O. M. 1985 Spectral and statistical properties of the equilibrium range in wind-generated gravity waves. *J. Fluid Mech.* **156**, 505–531.

PLANT, W. J. 1982 A relationship between wind stress and wave slope. *J. Geophys. Res.* **87**, 1961–1967.

TOBA, Y. 1973 Local balance in the air–sea boundary layer. III. On the spectrum of wind waves. *J. Oceanogr. Soc. Japan* **29**, 209–220.

ZAKHAROV, V. E. & FILONENKO, N. N. 1966 The energy spectrum for random surface waves. *Dokl. Akad. Nauk USSR* **170**, NG, 1291–1295.